



NUMERICAL INVESTIGATION UPON THE NO FORMATION IN H_2 -AIR IGNITION IN THE SUPERSONIC UNSTEADY SPATIAL MIXING LAYER

Adriana Ferreira de Faria

Milton Biage

Paulo Lopes Silva Júnior

Federal University of Uberlândia

Department of Mechanical Engineering

Uberlândia, M.G., Brazil

affaria@mecanica.ufu.br

Abstract. *In this work is analyzed the NO formation, as function of temperature, in diffusive turbulent flames of hydrogen, for such, are used detailed chemical and transport mechanisms and the complete two-dimensional governing equations in their conservative forms. The rates of the chemical reactions, the thermodynamic and transport properties are calculated by the softwares Chemkin and Package for Evaluation of the Transport Properties, both developed by Sandia National Laboratories. In this study the large eddy simulation technique is used and for solution of the system of equations, formed by the governing equations, it was applied the collocation spectral elements method with polynomials of Chebyshev. It was introduced a smoothing process, controlled by a sensor, to reduce the spurious oscillations in the numerical solution, in order to characterize the residual turbulence white noises were introduced. It was observed that there are not significant changes in the flow structure, in the level of concentration of the major intermediate species (O, OH and H) and in the NO concentration when the temperature of the fuel stream is increased.*

Key Words: *Supersonic Ignition, Combustion, Mixing Layer, and Supersonic Flow.*

1. INTRODUCTION

Most of combustion phenomena involve a very complex chemical network of interwoven elementary reactions. Because of the high value of the activation energy, the reaction rate is very sensitive to the temperature that varies under the heat released by the exothermic reactions. There are various approaches in modeling chemical reactions in hypersonic flows, namely, complete reaction, equilibrium kinetics and finite rate kinetics models. Here, it is adopted finite rate model, which tends to give reasonable results. The inclusion of finite rate chemistry results in the coupling of flow and species equations with source terms due to chemical reactions. This treatment involves significant complexity and increased computational time. (Linan and Crespo, 1976; Segal et al., 1995)

Considerable research in supersonic combustion has been performed in response to the interest in the development of scramjet engine for supersonic propulsion. The high speed

associated with the supersonic flow implies extremely short residence times for ignition to be effected. This is the major perceived difficulty in the development of scramjet technology. The other hand, an interesting recent theoretical result in the study of high speed chemically reacting mixing layers is that the significant amount of viscous heating can greatly facilitate the reaction rate and thereby the ignition event. Hence, the ignition can be facilitated by increasing flow speed, though the viscous conversion of the flow kinetic energy to thermal energy. (Im et al., 1996; Nishioka and Low, 1995; Waltrup, 1996)

Hydrogen is a strong candidate as a scramjet fuel because the limited residence time in the combustion chamber requires a fuel that has high energy density as well as high reactivity. Some analyses have been recently performed on ignition H_2 -Air. An important recognition which emerged from these studies is that while the high flow rate associated with the supersonic flow implies extremely short time residence for the ignition to be affected, the significant amount of viscous heating which takes place in a high sheared mixing layer can greatly facilitate the reaction rate and thereby the ignition event.

Increasing flow velocity of the air stream, the ignition distance first increasing linearly, due to simple residence time considerations. With further increasing in the air stream velocity, the ignition distance subsequently decreases Arrheniusly with the square of the Mach number in response to the significantly enhanced reaction rate due to the extensive amount of viscous heating. It can be defined two regimes of ignition from the critical temperature concept (the temperature which makes reaction rates of the chain branching reaction and the chain terminating reacting are equal, 924.70K for 1atm): high temperature and low temperature regimes. For all practical purposes, the ignition is not possible when the air temperature is lower than the temperature critical, that is in the low temperature regime, even allowing for the case where the viscous heating is important. (Im et al., 1993; Figueira da Silva et al., 1993; Nishioka and Law, 1995, Faria et al., 1998)

The choice of the chemical scheme is somewhat arbitrary and no significance qualitative difference in the flow structure was evidenced using different chemical schemes proposed in the literature, like seen in Figueira da Silva et al. (1993). However, it is important to analyze the NO and NO_2 concentrations in the supersonic combustion problems because they are the most arduous nitrogen oxides for the environment in the atmosphere. The NO_x are partially responsible for photochemical smog, corrosion of metals and reduction the growth of vegetation. The oxidation of NO to NO_2 is usually slow and must to be accelerated, then the NO is the dominant component of all NO_x produced.

The objective of this investigation is to analyze the NO formation, as function of temperature, in diffusive turbulent flames of hydrogen in supersonic mixing layer, in this manner it is necessary to use a chemical mechanism where the N_2 is treated as reagent and the NO and N are products. For this purpose, it is accomplished the numerical simulation of H_2 -air ignition in the supersonic unsteady mixing layer, with detailed transport and chemical reaction mechanisms and using the conservative form of the complete conservation equations. The chemical and transport properties are calculated by *Chemkin* and the *Transport Package*, respectively. To solve the problem it was used the collocation spectral element method with polynomials of Chebyshev like described in Canuto et al. (1988). This technique presents a high accuracy in the solution of the spatial derivatives, all calculation were made using the Gauss-Lobatto collocation points, with a grid of 121x105. The results are compared with those obtained by Figueira da Silva (1993) and Faria et al.(1998), where the chemical mechanism used consider the N_2 as inert chemical specie. In this study the large eddy simulation technique is used.

2. MATHEMATICAL FORMULATION

Generally, the governing equations are placed in their dimensionless forms, with the purpose of leaving them in function of parameters that characterize the flow, as the Reynolds, Prandtl, Lewis, Eckert and Schmidt numbers. An additional advantage in using the dimensionless equations is the fact that the variables are normalized, this way, their numerical values are in the prescribed limits.

The problem consists of a fast air stream and a slow fuel stream. The origin is located at the downstream edge of the thin splitter plate. The oxidizer and fuel streams are characterized by the following dimensional properties: U , T , ρ , μ , c_p , k and Y_k , these variables represent the streamwise velocity, temperature, density, viscosity, specific heat capacity in constant pressure, thermal conductivity of the mixture and mass fraction of the k^{th} species, with $k=0, \dots, N$ where N is the number of chemical species in the reacting flow. The symbols ∞ , $-\infty$ represent the air and fuel streams, respectively and the symbol $*$ represents the dimensional variables, the dimensionless variables are given by:

$$u_j = \frac{u_j^*}{U_\infty}, T = \frac{T^*}{T_\infty}, E = \frac{E^*}{U_\infty^2}, e = \frac{e^*}{U_\infty^2}, \rho = \frac{\rho^*}{\rho_\infty}, P = \frac{P^*}{\rho_\infty U_\infty^2}, t = \frac{2t^* U_\infty}{L_x}, \mu = \frac{\mu^*}{\mu_\infty}, k = \frac{k^*}{k_\infty}, c_p = \frac{c_p^*}{c_{p_\infty}}$$

$$w_k = \frac{w_k^* L_x}{\rho_\infty U_\infty}, \bar{V}_k^* = \frac{\bar{V}_k^* L_x}{D(O_2-N_2)_\infty}, D_k = \frac{D_k^*}{D(O_2-N_2)_\infty}, D_k^T = \frac{D_k^{T*}}{D(O_2-N_2)_\infty \rho_\infty} \quad (1 \text{ to } 15)$$

P , E and e are the pressure, total energy and internal energy of the system, D_k , D_k^T , \bar{V}_k and w_k are the mass diffusion and thermal diffusion coefficients, diffusion velocity and mass production rate of the k^{th} species. The length of the domain in the x^* direction is L_x , $-L_x/2 \leq x^* \leq L_x/2$ and in the y^* direction is L_y , $-L_y/2 \leq y^* \leq L_y/2$.

The system of dimensionless governing equations has the following vectorial form:

$$\frac{\partial U}{\partial t} + \frac{L_x}{(\Delta x^*)_i} \frac{\partial E}{\partial x} + \frac{L_x}{(\Delta y^*)_j} \frac{\partial F}{\partial y} = S, \quad U = \begin{pmatrix} \rho \\ \rho u \\ \rho v \\ \rho E \\ \rho Y_k \end{pmatrix}, \quad S = \begin{pmatrix} 0 \\ 0 \\ 0 \\ 0 \\ w_k \end{pmatrix} \quad (16, 17, 18)$$

$$E = \begin{pmatrix} \rho u \\ \rho u u + P - \frac{1}{Re \delta_0} \tau_{xx} \\ \rho v u - \frac{1}{Re \delta_0} \tau_{xy} \\ \rho u E + \frac{1}{Pe} q_x + P u - \frac{1}{Re \delta_0} (\tau_{xx} u + \tau_{xy} v) \\ \rho u Y_k + \frac{1}{Re \delta_0} \frac{1}{Sc} J_{kx} \end{pmatrix}, \quad F = \begin{pmatrix} \rho v \\ \rho u v - \frac{1}{Re \delta_0} \tau_{xy} \\ \rho v v + P - \frac{1}{Re \delta_0} \tau_{yy} \\ \rho v E + \frac{1}{Pe} q_y + P v - \frac{1}{Re \delta_0} (\tau_{xy} u + \tau_{yy} v) \\ \rho v Y_k + \frac{1}{Re \delta_0} \frac{1}{Sc} J_{ky} \end{pmatrix} \quad (19, 20)$$

Where $(\Delta x^*)_i$ and $(\Delta y^*)_j$ are the lengths of each spectral element in the directions x^* and y^* , respectively, with $i=1, \dots, Ne_x$ and $j=1, \dots, Ne_y$, where Ne_x and Ne_y are the number of elements in the directions x^* and y^* , respectively. Re_δ is the Reynolds number defined for δ_0 , where δ_0 is the thickness of mixing layer, Sc , Pr and Pe are the Schmidt, Prandtl and Peclet numbers. The components of the mean strain tensor for a Newtonian fluid, τ_{ij} , the components of the heat flux vector, \bar{q} , and mass flux vector, \bar{J}_k are:

$$\tau_{xx} = (2\delta_0) \frac{2}{3} \mu \left(\frac{2}{(\Delta x^*)_i} \frac{\partial u}{\partial x} + \frac{1}{(\Delta y^*)_j} \frac{\partial v}{\partial y} \right), \quad \tau_{yy} = (2\delta_0) \frac{2}{3} \mu \left(\frac{2}{(\Delta y^*)_j} \frac{\partial v}{\partial y} - \frac{1}{(\Delta x^*)_i} \frac{\partial u}{\partial x} \right) \quad (21, 22)$$

$$\tau_{xy} = (2\delta_0) \mu \left(\frac{1}{(\Delta x^*)_i} \frac{\partial u}{\partial x} + \frac{1}{(\Delta y^*)_j} \frac{\partial v}{\partial y} \right) \quad (23)$$

$$(q_c)_x = 2\delta_0 \left(\frac{k}{Ec} \right) \frac{1}{(\Delta x^*)_i} \frac{\partial T}{\partial x} + Le \sum_{k=1}^N h_k (J_k)_x, \quad (q_c)_y = 2\delta_0 \left(\frac{k}{Ec} \right) \frac{1}{(\Delta y^*)_j} \frac{\partial T}{\partial y} + Le \sum_{k=1}^N h_k (J_k)_y \quad (24, 25)$$

$$\bar{J}_k = 2\delta_0 \rho Y_k \bar{V}_k \quad (26)$$

Le is the Lewis number, The dimensionless diffusion velocity of the k^{th} specie, \bar{V}_k is:

$$(V_k)_x = -\frac{1}{X_k} D_{km} (d_k)_x - \frac{D_k^T}{\rho Y_k T} \frac{1}{(\Delta x^*)_i} \frac{\partial T}{\partial x}, \quad (V_k)_y = -\frac{1}{X_k} D_{km} (d_k)_y - \frac{D_k^T}{\rho Y_k T} \frac{1}{(\Delta y^*)_j} \frac{\partial T}{\partial y} \quad (27, 28)$$

$$(d_k)_x = \frac{1}{(\Delta x^*)_i} \left(\frac{\partial X_k}{\partial x} + (X_k - Y_k) \frac{1}{P} \frac{\partial P}{\partial x} \right), \quad (d_k)_y = \frac{1}{(\Delta y^*)_j} \left(\frac{\partial X_k}{\partial y} + (X_k - Y_k) \frac{1}{P} \frac{\partial P}{\partial y} \right) \quad (29, 30)$$

X_k is molar fraction of the k^{th} specie. In compressible flows become necessary to establish a relation between pressure, temperature, density and internal energy, which is given by theory of ideal gases, where $\gamma = c_p / c_v$ and Ec is the Eckert number.

$$P = \rho (\gamma - 1) \bar{e}, \quad T = Ec \gamma \frac{\bar{e}}{c_v} \quad (31, 32)$$

where

$$\bar{e}^*(T^*) = e^*(T^*) - \sum_{k=1}^N Y_k e_k^0(0) = c_v^* T^* \quad (33)$$

The initial conditions

$$u(x, y, t=0) = [U_o + U_l \tanh(y^* / \delta_0)] / U_\infty, \quad v(x, y, t=0) = 0 \quad (34, 35)$$

$$T(x, y, t=0) = [T_o + T_l \tanh(y^* / \delta_0)] / T_\infty \quad (36)$$

$$\rho(x, y, t=0) = [f(T(x, y^*, t^*=0), Y_k(x, y^*, t^*=0), P_\infty = 1 \text{ atm.})] / \rho_\infty \quad (37)$$

$$Y_k(x, y, t=0) = Y_{k_o} + Y_{k_l} \tanh(y^* / \delta_0), \quad k=1, \dots, N \quad (38)$$

where:

$$U_o = \frac{U_\infty + U_{-\infty}}{2}, \quad U_I = \frac{U_\infty - U_{-\infty}}{2}, \quad T_o = \frac{T_\infty + T_{-\infty}}{2} \quad (39, 40, 41)$$

$$T_I = \frac{T_\infty - T_{-\infty}}{2}, \quad Y_{k_o} = \frac{Y_{k_\infty} + Y_{k_{-\infty}}}{2}, \quad Y_{k_I} = \frac{Y_{k_\infty} - Y_{k_{-\infty}}}{2} \quad (42, 43, 44)$$

The Boundary conditions

x- direction:

$$u(x = -l, y, t) = [\bar{u}(y^*) + f(y^*)\varepsilon\hat{V}(y^*, t^*)] / U_\infty, \quad v(x = -l, y, t) = [f(y^*)\varepsilon\hat{V}(y^*, t^*)] / U_\infty \quad (45, 46)$$

$$T(x = -l, y, t) = [T_o + T_I \tanh(y^* / \delta_0)] / T_\infty \quad (47)$$

$$\rho(x = -l, y, t = 0) = [f(T(x, y^*, t^* = 0), Y_k(x, y^*, t^* = 0), P_\infty)] / \rho_\infty \quad (48)$$

$$Y_k(x = -l, y, t = 0) = Y_{k_o} + Y_{k_I} \tanh(y^* / \delta_0), k = 1, \dots, N \quad (49)$$

$$\frac{\partial \varphi(x = l, y, t)}{\partial x} = 0, \quad \varphi = \{u, v, E, \rho, Y_k\} \quad (50)$$

y-direction:

$$u(x, y = l, t) = l, \quad v(x, y = l, t) = 0, \quad T(x, y = l, t) = l, \quad \rho(x, y = l, t = 0) = l, \quad Y_k(x, y = l, t) = Y_{k_\infty} \quad (51 \text{ to } 55)$$

$$u(x, y = -l, t) = \frac{U_{-\infty}}{U_\infty}, \quad v(x, y = -l, t) = 0, \quad T(x, y = -l, t) = \frac{T_{-\infty}}{T_\infty}, \quad \rho(x, y = -l, t = 0) = \frac{\rho_{-\infty}}{\rho_\infty}$$

$$Y_k(x, y = -l, t) = Y_{k_{-\infty}} \quad (56 \text{ to } 60)$$

$\hat{V}(y^*, t^*)$ is a random number, which constitutes a centered and reduced white noise perturbation. This white noise will inject the same small amount of energy into all the longitudinal modes of the basic flow. ε is the amplitude of the random perturbation, the function $f(y^*)$ represents a Gaussian filter modulating the amplitude of the perturbations, which confines all the perturbations of the basic flow to its rotational zone. (Comte et al, 1989; Faria et al., 1998)

3 - CHEMICAL SCHEME

The chemical kinetics scheme used in this work is the one proposed by Kee et al. (1989), and is given in Table 1. In this chemical scheme N_2 is treated as a reagent, and the chemical species considered are: $H_2, O_2, N_2, H_2O, O, OH, H, HO_2, H_2O_2, N$ and NO and there are 23 elementary chemical reaction in this mechanism. The rates of the chemical reactions, the thermodynamic and transport properties are calculated by the softwares *Chemkin* and *Package for Evaluation of the Transport Properties*, both developed by *Sandia National Laboratories*.

Table 1. Gas Phase Mechanism of Hydrogen Oxidation, $k_{fi} = A_i(T)^{\beta_i} \exp(-E_i / R_c T)$.

Reaction	$A_i(\text{cm, mol, s})$	β_i	$E_i(\text{cal/mol})$
1. $\text{H}_2 + \text{O}_2 \Leftrightarrow 2\text{OH}$	0.170E+14	0.00	47780
2. $\text{OH} + \text{H}_2 \Leftrightarrow \text{H}_2\text{O} + \text{H}$	0.117E+10	1.30	3626
3. $\text{O} + \text{OH} \Leftrightarrow \text{O}_2 + \text{H}$	0.4000E+15	-0.50	0
4. $\text{O} + \text{H}_2 \Leftrightarrow \text{OH} + \text{H}$	0.506E+05	2.67	6290
5. $\text{H} + \text{O}_2 + \text{M} \Leftrightarrow \text{HO}_2 + \text{M}^a$	0.361E+18	-0.72	0
6. $\text{OH} + \text{HO}_2 \Leftrightarrow \text{H}_2\text{O} + \text{O}_2$	0.750E+13	0.00	0
7. $\text{H} + \text{HO}_2 \Leftrightarrow 2\text{OH}$	0.140E+15	0.00	1073
8. $\text{O} + \text{HO}_2 \Leftrightarrow \text{O}_2 + \text{OH}$	0.140E+14	0.00	1073
9. $2\text{OH} \Leftrightarrow \text{O} + \text{H}_2\text{O}_2$	0.600E+09	1.30	0
10. $\text{H} + \text{H} + \text{M} \Leftrightarrow \text{H}_2 + \text{M}^b$	0.100E+19	-1.00	0
11. $\text{H} + \text{H} + \text{H}_2 \Leftrightarrow \text{H}_2 + \text{H}_2$	0.920E+17	-0.60	0
12. $\text{H} + \text{H} + \text{H}_2\text{O} \Leftrightarrow \text{H}_2 + \text{H}_2\text{O}$	0.600E+20	-1.25	0
13. $\text{H} + \text{OH} + \text{M} \Leftrightarrow \text{H}_2\text{O} + \text{M}^c$	0.160E+23	-2.00	0
14. $\text{H} + \text{O} + \text{M} \Leftrightarrow \text{OH} + \text{M}^d$	0.620E+17	-0.60	0
15. $\text{O} + \text{O} + \text{M} \Leftrightarrow \text{O}_2 + \text{M}$	0.189E+14	0.00	-1780
16. $\text{H} + \text{HO}_2 \Leftrightarrow \text{H}_2 + \text{O}_2$	0.125E+14	0.00	0
17. $\text{HO}_2 + \text{HO}_2 \Leftrightarrow \text{H}_2\text{O}_2 + \text{O}_2$	0.200E+13	0.00	0
18. $\text{H}_2\text{O}_2 + \text{M} \Leftrightarrow \text{OH} + \text{OH} + \text{M}$	0.130E+18	0.00	45500
19. $\text{H}_2\text{O}_2 + \text{H} \Leftrightarrow \text{HO}_2 + \text{H}_2$	0.160E+13	0.00	3800
20. $\text{H}_2\text{O}_2 + \text{OH} \Leftrightarrow \text{H}_2\text{O} + \text{HO}_2$	0.100E+14	0.00	1800
21. $\text{O} + \text{N}_2 \Leftrightarrow \text{NO} + \text{N}$	0.140E+15	0.00	75800
22. $\text{N} + \text{O}_2 \Leftrightarrow \text{NO} + \text{O}$	0.6400E+10	1.00	6280
23. $\text{OH} + \text{N} \Leftrightarrow \text{NO} + \text{H}$	0.400E+14	0.00	0.0

a: $\alpha_{\text{H}_2\text{O}}=18.6$, $\alpha_{\text{H}_2}=2.86$, $\alpha_{\text{N}_2}=1.26$; b: $\alpha_{\text{H}_2\text{O}}=0.0$, $\alpha_{\text{H}_2}=0.0$; c: $\alpha_{\text{H}_2\text{O}}=5$; d: $\alpha_{\text{H}_2\text{O}}=5$

4. NUMERICAL METHOD

For solution of system of equations it was applied the Collocation Spectral Elements Method with polynomials of Chebyshev for spatial discretization and time stepping procedure with multi-stages for time discretization (Runge-Kutta). Considering that the roundoff error generates substantial oscillations in the vicinity of discontinuities in the flow properties, we used an exponential filter to smooth the variables, with aid of a sensor. This technique presented a high accuracy in the calculation of the spatial derivatives that was determined by Chebyshev transform (Canuto et al., 1988). The computational code was built with aim to achieve quickly the stationary solution of turbulent compressible flows.

In this study all calculation were made using the Gauss-Lobatto collocation points, with a grid of 121x105. The physical domain length was established so that the lateral boundary conditions did not affect the development the mixing region necessary for the combustion

processes. Also, the axial length was set up such as the reacting mechanisms attained a uniform spatial evolution. Normally, the structure of the spatial mixing layer for either reacting or homogenous flows depends significantly of the initial thickness vorticity. However, in this study one did not analyze the influence of this property. The results presented in this paper were obtained with $\delta_0=0.01\text{m}$. The level of the random noise was set up with order 10^{-2} .

A major advance in understanding turbulent shear flow was the discovery that important aspects of the flow processes in a shear layer are dominated by large scale organized structures and that species transport in the shear layer is dominated by these structures. All statistical models used for turbulence modeling have basic limitations because of the non-linear, non-local and non-Gaussian properties of turbulence. On the other hand, the direct numerical simulation is limited because of the large range of space and time scales involved in the problems. Both approaches are successful for limited applications but the ideal solution to turbulence modeling, at present, seems to be their combination, i.e. the Large Eddy Simulation (LES). The definition of what is called of large eddies and what the subgrid-scale motions is not trivial and deserves special discussion in the literature. In this work we can say that the smoothing process performs like a subgrid-scale model, thereby the Large Eddy Simulation technique was applied. (Schumann, 1991)

5. RESULTS

It is important in combustion study to verify the dependence of ignition distance on the various system parameters like temperature and velocity of fuel, oxidizer and pressure. However, in this paper we want to know the variation of *NO* concentration as a function of temperature and to verify, also, the importance of this variable in chemical reactions.

The Figure 1 represents some combustion results, where the fast air stream was 5400m/s and 1200K and the slow fuel stream was 3000m/s and 500K. In a similar manner, the Figure 2 represents an air stream with 1200K and 5400m/s and a fuel stream with 1200K and 3000m/s. The Figure 1 represents the case 1, while the Figure 2 represents the case 2. The physical domain is: $-30 \leq x^* \leq 30\text{cm}$ and $-20 \leq y^* \leq 20\text{cm}$. These figures illustrate both the flow dynamic and combustion behaviors. Like it was described in Faria et al. (1998), the combustion is found to develop first on the air side of the mixing layer, as can be remarked on the all graphics in Figures 1 and 2. It is observed, also, on the Figures 1a and 2a, which represent the transversal velocity evolution, that the flow is perturbed more intensely in a region comprise into the fuel stream layer, with lower velocity than the stream oxidizer layer. Clearly, we can affirm that flow disturbed region is defined by a Mach cone with origin close to the trailing edge of the splitter plate. This flow aspect was described in detail in previous paper (Faria et al., 1998), however, even it was changed the actual chemical mechanism, using the reactions involving the N_2 as reagent and *NO* and *N* as products, this flow features was not practically changed.

The Figures 3 and 4 show the chemical species and temperature profile for the case 1 and 2, respectively. The Figure 3a represents the reactants transverse profile at streamwise position $x^*=0.0\text{cm}$. We observe the excess of oxygen that is present in the H_2 -air of the mixing layer, in a position after the ignition point. One can also see this structure in figure 1c. This fact characterizes a rich premixed H_2 -air combustion zone. It should be noticed that a similar structure is not found in the lean side of the mixing layer due to the large diffusion velocity of H_2 , this results is in conformity with that described by Figueira da Silva et al. (1993). This fact can be also observed in the figure 4a for the case 2. In this figures, 3a and 4^a, it is observed that there is not a significantly change in N_2 concentration in the mixing layer region.

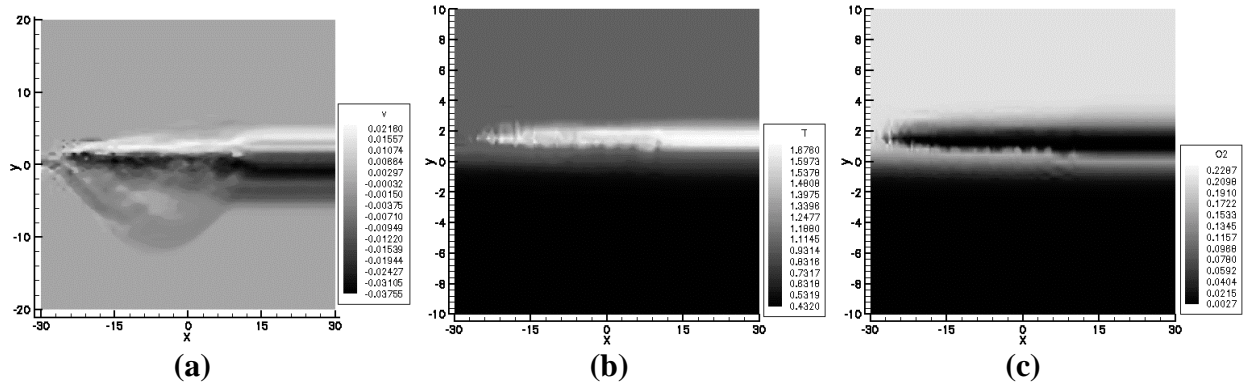


Figure 1 – Property fields at $t=1.5089$, $U_\infty=5400\text{m/s}$, $U_{-\infty}=3000\text{m/s}$, $T_\infty=1200\text{K}$ and $T_{-\infty}=500\text{K}$.
(a) v , (b) T , (c) O_2 .

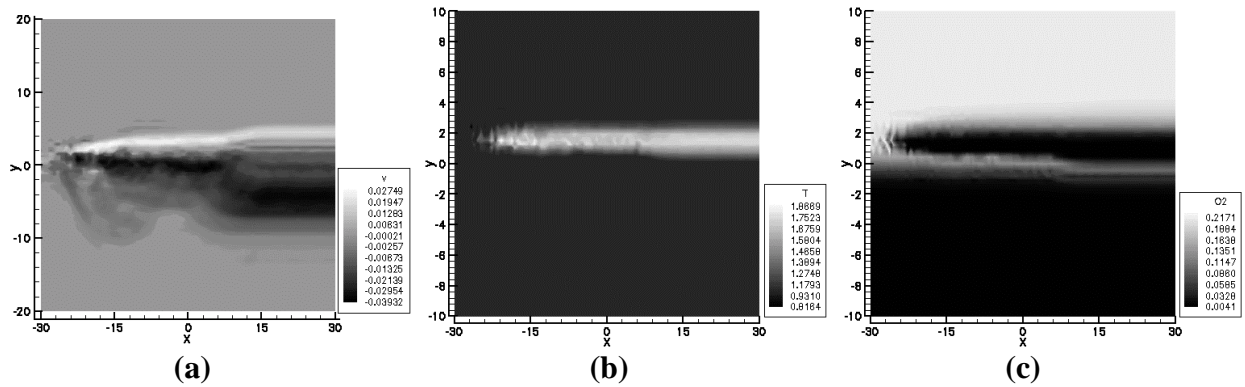


Figure 2 – Property fields at $t=1.5071$, $U_\infty=5400\text{m/s}$, $U_{-\infty}=3000\text{m/s}$, $T_\infty=1200\text{K}$ and $T_{-\infty}=1200\text{K}$.
(a) v , (b) T , (c) O_2 .

The Figures 3b and 4b show the mass fraction profile for the major intermediate chemical species, O , OH and H , while the Figures 3c and 3b illustrate H_2O mass fraction profile. The level of concentration of the species obtained in this work are almost the same if it is compared with the results obtained in Figueira da Silva et al. (1993) and Faria et al. (1998), where the mechanism used did not consider the reactions involving the N_2 . We can note that while the levels of concentrations of the major intermediate chemical species are of the 10^{-2} order, the NO concentration is 10^{-7} , Figure 3d and 4d. It is also important to say that even if the temperature of fuel stream is increased, it is not observed significantly change in the flow structure behavior and in the level of concentration of this chemical species.

We can observe the temperature level in the mixing layer in the Figures 3e and 4e, for the case 1 and 2, respectively. These figures represent temperature transverse profile for $x^*=0.0\text{cm}$, for different step time. One can observe in the Figures 3f and 4f, following the streamwise directions, for $y^*=1.5533\text{cm}$, different regions in the flow. First, an induction region, where the temperature remaining quasi-constant. We can note that this region is smaller for the case 2. After there is a thermal runaway region, where we define the ignition point like been $x^*=-10\text{cm}$ for the case 1 and $x^*=-28\text{cm}$ for the case 2. This shows that an efficient way to decrease the ignition distance is increasing the temperature of fuel stream. Figueira da Silva et al. (1993) identify an induction region, a thermal runaway region, a region where both premixed combustion and diffusion flame coexist and diffusion flame region. In their work, classical boundary layer approximations, in steady state, are used.

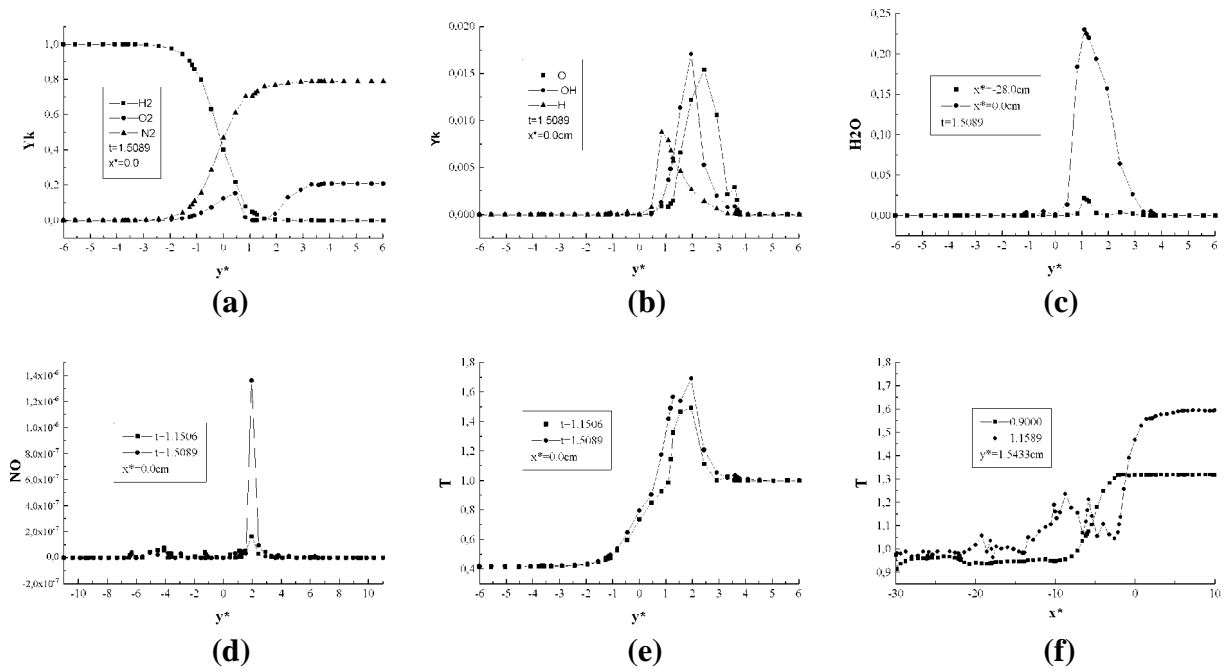


Figure 3 – Chemical species and temperature profiles, $U_{\infty}=5400\text{m/s}$, $U_{\infty}=3000\text{m/s}$, $T_{\infty}=1200\text{K}$ and $T_{\infty}=500\text{K}$.

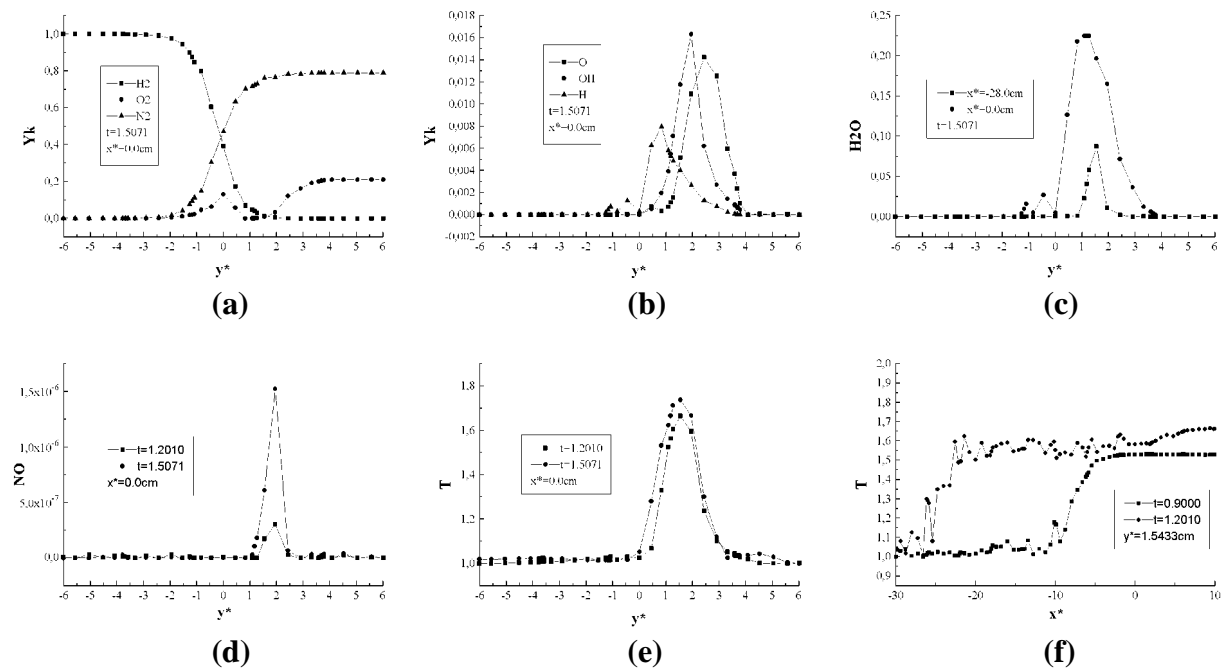


Figure 4 – Chemical species and temperature profiles, $U_{\infty}=5400\text{m/s}$, $U_{\infty}=3000\text{m/s}$, $T_{\infty}=1200\text{K}$ and $T_{\infty}=1200\text{K}$.

The basic structure of the combustion phenomena, showed in this work, appears to be analogous to that described by Figueira da Silva et al. (1993), Nishioka and Law (1995) and Faria et al. (1998), however, more results for different stream conditions must be analyzed and treated statically. It is important to verify the dependence of ignition distance on the various system parameters like, Mach, Reynolds, Peclet and Schmidt numbers, temperature of fuel and oxidizer, and pressure.

REFERENCES

- Canuto, C., Hussaini, M. Y., Quarteroni, A. and Zang, T. A., 1988. *Spectral methods in fluid dynamics*. Springer-Verlag.
- Comte, P., Lesieur, M., Laroche, H. and Normand, X., 1989. Numerical simulations of turbulent plane shear layers. *Turbulent Shear Flow*, 6, 360-380.
- Faria, A. F., Biage, M., Júnior, P.L.S., 1998. Simulation of ignition in supersonic H₂-air unsteady mixing layer using spectral method. *VII ENCIT*, 1, 126-131.
- Figueira da Silva, L. F., Deshaies, B., Champion, M and Rene-Corail, M., 1993. Some specific aspects of combustion in supersonic H₂-air laminar mixing layers. *Combustion Science and Technology*, 89, 317-333.
- Im, H. G. and Bechold, J. K., 1993. Analysis of thermal ignition in supersonic flat plate boundary layers. *Journal Fluid Mech.*, 249, 99-120.
- Im, H. G., Helenbrook, B. T., Lee, S. R. and Law, C. K., 1996. Ignition in the supersonic hydrogen-air mixing layer with reduced reaction mechanisms. *Journal Fluid Mech.*, 322, 275-296.
- Kee, R. J., Rupley, F. M. and Miller, J. A., 1989. Chemkin-II: A Fortran chemical kinetics package for the analysis of gas phase chemical kinetics. *SANDIA REPORT*, SAND89-8009B UC706.
- Law, C. K., 1994. *Combustion Theory*. Princeton University.
- Linan, A. and Crespo, A., 1976. An asymptotic analysis of unsteady diffusion flames for large activation energies. *Combustion Science and Technology*, 14, 95-110.
- Nishioka, M. and Law, C. K., 1995. A numerical study of ignition in the supersonic H₂-air laminar mixing layer. *AIAA*, Paper 95-0377.
- Schumann, U., 1991. *Direct and Large Eddy Simulation of Turbulence*. von Karman Institute for Fluid Dynamics.
- Segal, C., Hariri, H. and McDaniel, J. C., 1995. Effects of the chemical reaction model on calculations of supersonic combustion flows. *J. Propul.-Power*, 11(03), 565-568.
- Waltrup, P. J., 1996. Liquid fuel supersonic combustion ramjets, present and future. *AIAA*, Paper 86-1158.
- Williams, F. A., 1965. *Combustion Theory*. Addison - Wesley Publishing Company.